



**HAL**  
open science

## Modelling of weld inspection by using a paraxial ray-tracing

Nicolas Leymarie, Audrey Gardahaut, Karim Jezzine, Ekaterina Iakovleva,  
Bertrand Chassignole, Fabienne Rupin

► **To cite this version:**

Nicolas Leymarie, Audrey Gardahaut, Karim Jezzine, Ekaterina Iakovleva, Bertrand Chassignole, et al.. Modelling of weld inspection by using a paraxial ray-tracing. NDT 2013 - 52nd British Institute of Non-destructive Testing Annual Conference, Sep 2013, Telford, United Kingdom. hal-04510045

**HAL Id: hal-04510045**

**<https://hal.science/hal-04510045>**

Submitted on 18 Mar 2024

**HAL** is a multi-disciplinary open access archive for the deposit and dissemination of scientific research documents, whether they are published or not. The documents may come from teaching and research institutions in France or abroad, or from public or private research centers.

L'archive ouverte pluridisciplinaire **HAL**, est destinée au dépôt et à la diffusion de documents scientifiques de niveau recherche, publiés ou non, émanant des établissements d'enseignement et de recherche français ou étrangers, des laboratoires publics ou privés.

# Modelling of weld inspection by using a paraxial ray-tracing

N. Leymarie, A. Gardahaut, K. Jezzine, E. Iakovleva  
CEA, LIST,  
91191 Gif-sur-Yvette Cedex, France  
33-1-69-08-60-35  
33-1-69-08-75-97  
[nicolas.leymarie@cea.fr](mailto:nicolas.leymarie@cea.fr)

Bertrand Chassignole, Fabienne Rupin  
EDF R&D  
Moret sur Loing, 77818, France

## Abstract

The controllability of welded joints is a major industrial challenge to meet the requirements of safety and service life of structures. Nevertheless, in most of austenitic welds, ultrasonic detection performances decrease due to unfavourable wave interactions with microstructure. The understanding of such phenomena requires the use of accurate numerical models. In particular, the ray-based model implemented in CIVA can simulate weld inspections considering heterogeneous and anisotropic materials where the microstructure is described using several homogeneous domains. However, according to the size of the domains and the impedance contrast between neighbouring domains, such weld descriptions may lead to discrepancies between simulations and experimental results. To overcome this difficulty, the extension to smoothly inhomogeneous anisotropic media may be performed by using paraxial ray tracing. In this paper, simulation results obtained with this method are presented and compared to finite elements and experimental data on a well-documented sample representative of a weld located in the primary circuit of nuclear power plants.

This work is a part of the MOSAICS project, supported by the ANR (French National Research Agency) which aims at significantly improving the understanding of the influence of the weld structure on the performance of ultrasonic NDT inspections.

## 1. Introduction

The MOSAICS project, supported by the ANR (French National Research Agency), brings together various partners around the modelling of ultrasonic testing on austenitic welds taking into account complex 3D configurations. A general paper of this conference presents the different contributions of all the partners in this project <sup>(1)</sup>.

Austenitic multi-pass welds are characterized by anisotropic and heterogeneous structures which generate a lot of disturbances of the ultrasonic beam during an inspection. Different approaches have been proposed to model the propagation of ultrasonic waves in such anisotropic media. In particular, finite element method has been used by Chassignole and coll.<sup>(2,3)</sup> (ATHENA code) to simulate the wave propagation in welds. Alternatively, semi-analytical propagation models based on ray theory have been implemented in the CIVA software<sup>(4,5)</sup> and applied to weld inspection. In these previous studies, the weld is described as a set of several anisotropic homogeneous domains with a given crystallographic orientation. Nevertheless, if the domains are small compared to the wavelength and exhibit strong variations in grain orientation, a chaotic behaviour of rays may be observed, leading to inaccurate results<sup>(6)</sup>. To overcome this problem, the weld can be considered as a unique domain in which the variation of grain orientation is described through a spatial mapping of crystallographic orientations in the weld. This paper focus on this new modelling approach by using a ray-based model well suited for a smoothly inhomogeneous anisotropic medium. Based on a grain orientation mapping, this simulation model is validated by comparison with finite elements results in 2D. Then, 3D calculations are performed and compared with experimental data obtained on a specific welded mock-up containing calibrated flaws on a sample representative of a weld located in the primary circuit of nuclear power plants.

## **2. Simulation of ultrasonic beam propagation in CIVA thanks to a grain orientation mapping of the weld**

### ***2.1 Description of the weld properties***

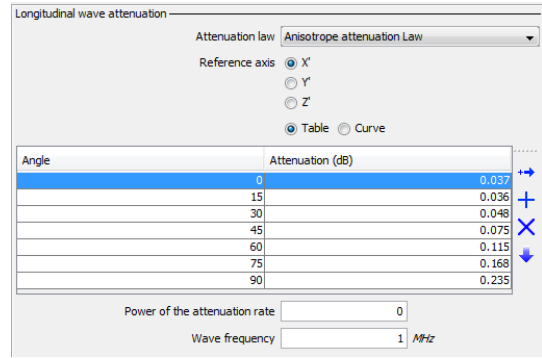
To perform the simulation of the wave propagation in the weld, the mechanical properties at any position in the weld are required. For a given grain orientation, we assume that the weld properties are constant and expressed with a complex stiffness tensor of an orthotropic material whose grain axis is normal to a plane of symmetry. The weld is then fully described considering:

- a complex orthotropic stiffness tensor obtained by using an ultrasonic measurements device designed in order to simultaneously determine the elastic properties and the attenuation coefficients of the wave in an anisotropic weld <sup>(1)</sup>
- a mapping of the grain orientation with respect to the location in the weld obtained from metallographic and crystallographic analyses including image processing, X-Ray diffraction and Electron BackScattering Diffraction (EBSD) techniques.

Except for the attenuation coefficients, all these data are taken into account in a prototype version of CIVA. Concerning the attenuation coefficients, only anisotropy of attenuation in a plane of symmetry containing grain axis is currently considered. The general anisotropy of the wave attenuation should be handled subsequently before the end of the project.

As illustrated in figure 1, the real part of the stiffness matrix is classically defined in a 6 by 6 table and the attenuation properties are expressed in a two columns table given the attenuation with respect to the wavefront direction. This direction, expressed in a plane, is defined by an angle with respect to a reference axis corresponding in our case to the grain orientation (see figure 1-b).

Density		7.915 $g.cm^{-3}$	
Symmetry		Orthotropic	
Anisotropic matrix (GPa)			
218	148	148	0
148	248	110	0
148	110	248	0
0	0	0	80
0	0	0	105
0	0	0	105

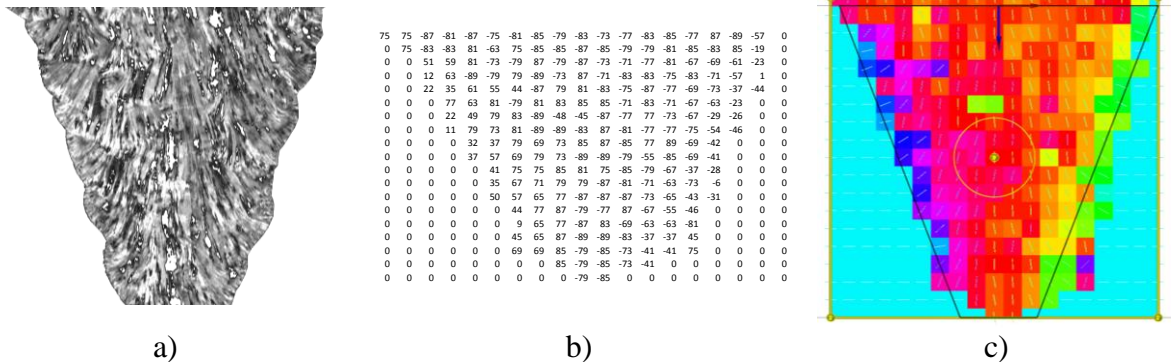


a)

b)

**Figure 1. Graphic user interface used in CIVA to define: a) the anisotropic elastic properties and b) the anisotropic behaviour of the wave attenuation in the weld.**

The mapping of the grain orientation is given by the way of a formatted text file. This file contains the angles of the grain orientation with respect to the X axis, expressed as a N by M table. This discrete description of the crystallographic orientation in a weld can be obtained by applying image processing techniques on the macrography<sup>(7)</sup>. In the Graphic User Interface (GUI) of CIVA, this file can be loaded and is also interpreted as an image whose dimensions and position could be fixed by the user in the scene including the welded sample (see figure 2).



a)

b)

c)

**Figure 2. Definition of the grain orientation in a welding joint in CIVA: a) example of macrography of the weld; b) corresponding formatted text file with grain orientation angles; c) discrete description of the crystallographic orientation illustrated in the CIVA scene.**

## 2.2 Extension of the paraxial ray tracing model used in CIVA: adaptation with the mapping description

The simulation of wave propagation implemented in CIVA is based on the Dynamic Ray Tracing model<sup>(8)</sup> (DRT) and is currently limited to anisotropic homogeneous domains. To adapt this model to the mapping description of the weld, an extension of the DRT technique has been developed. Using cubic spline interpolation on the grid of the mapping, a smoothly inhomogeneous representation of the welding medium can be considered. Hence, we obtain a continuously varying description for which the DRT model can be extended.

To derive the approximate high-frequency expressions for body waves propagating in smoothly varying media, the approach used is based on a generalization of the approach

used for homogeneous media by solving two differential ray tracing systems. From the eikonal equation<sup>(8)</sup>, the axial ray system is used to evaluate the ray trajectory and is composed of two coupled ordinary differential equations describing the variations of the position  $x_i$  and the slowness  $p_i$  with respect to the travel time  $T$ :

$$\begin{cases} \frac{dx_i}{dT} = a_{ijkl} p_l g_j g_k = V_i^e, \\ \frac{dp_i}{dT} = -\frac{1}{2} \frac{\partial a_{ijkl}}{\partial x_i} p_k p_n g_j g_l, \end{cases} \dots\dots\dots (1)$$

where  $a_{ijkl}$  are the components of the elasticity tensor of the medium normalized by its density,  $g_j$  are polarization components associated with the slowness vector of the wave mode. In the first equation concerning the ray trajectory, we recognize the expression of the energy velocity denoted  $V_i^e$ . In the second expression, the perturbation of the slowness components is related to spatial variation of the elasticity tensor and can be interpreted as a continuous refraction along the trajectory of the wavefront.

The second system, called paraxial ray system, describes the evolution of the ray tube with respect to the axial ray. Assuming that the transport equation imposes the conservation of the energy flux across a ray tube section<sup>(8)</sup>, the amplitude of the propagating rays can also be estimated in any inhomogeneous anisotropic media. The notations being complex, the corresponding equations are not developed in this article. More details are provided in a recent communication to be published<sup>(9)</sup>.

The numerical solution of both axial and paraxial ray tracing systems can be performed using various methods such as the Euler or Runge-Kutta methods. As a first study, we have chosen to use the Euler method. If the numerical performance of this first-order scheme is worse than for other higher order schemes, the accuracy of the ray tracing can be more easily controlled. Once the method is validated, the use of higher-order schemes will then improve the numerical performance of the method.

### 3. Validation of the DRT model on a mapping weld description by comparison with FE calculation

In a recent study<sup>(9)</sup>, the paraxial ray tracing method has been validated for a simplified description of a V-shaped weld with grain orientation described by a closed-form expression proposed by Ogilvy<sup>(10)</sup>.

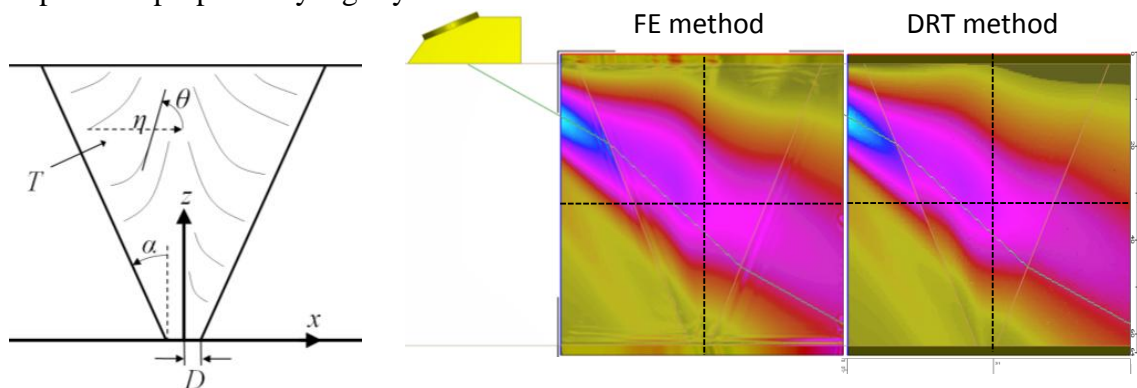


**Figure 3. Comparison of maximum particle velocity obtained with a FE code (ATHENA) and a DRT model for a weld described by a closed-form expression.**

In this case, the closed-form provides a perfect smooth description of the weld properties. As shown in figure 3, the results obtained with a FE code (ATHENA) and the DRT method are similar. This ideal case validates the DRT model itself. However, a closed-form expression of grain orientation cannot be used for any realistic cases. The mapping description of grain orientations is therefore an alternative to treat realistic welding joints.

In order to obtain a smooth variation of elastic properties of the weld, we have chosen to evaluate properties with cubic spline interpolation. Therefore, first and second derivatives of elastic properties with respect to the spatial position in the weld are continuous. Hence, the numerical resolution of axial and paraxial schemes should be more stable. A comparison between FE and DRT models was done on the previous description (see figure 2) obtain from image processing on weld macrograph. The results, illustrated in figure 4, are not as good as for the case of a closed-form description.

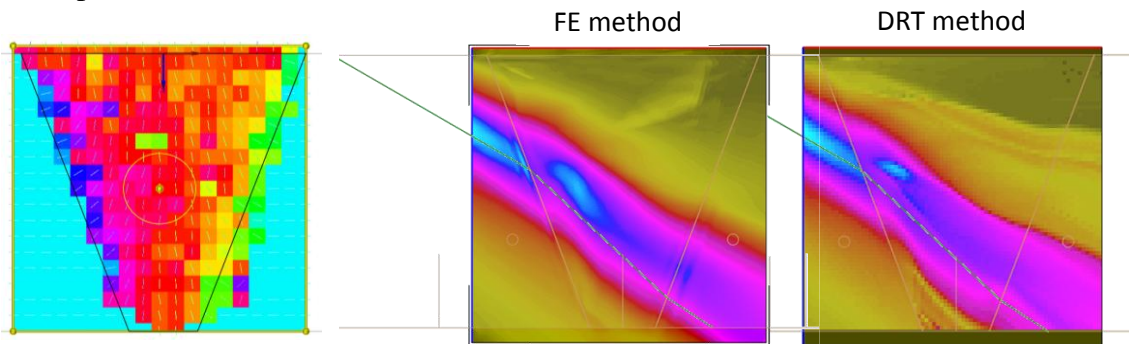


**Figure 4. Comparison of maximum particle velocity obtained with a FE code and a DRT model in a welding joint described with a mapping of grain orientation.**

If the results in figure 4 seem to look worse, the comparison of the amplitude curves along the two axes of the weld (see in figure 5) shows differences below 1.5 dB.

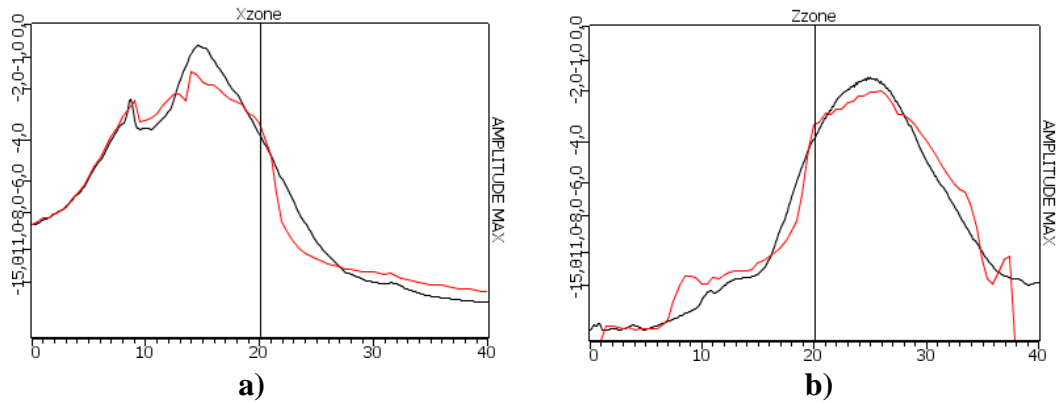


**Figure 5. Values of the maximum particle velocity in the middle of the 2D zone illustrated in figure 4 (mapping description of the weld): a) with respect to X position (Z fixed in the middle) b) with respect to Z position (X fixed in the middle) for FE results in black and a DRT results in red.**

The observed discrepancies could be due to the interpolation close to the boundary of the welding medium. In this area, the interpolation is very sensitive to the position of the mapping with respect to sample defined in the CIVA scene. The positioning being

currently done manually, a small difference may change strongly the derivative values of elastic properties close to the boundary of welding joint and alter consequently the calculation of wave refraction. Studies are currently in progress to evaluate this sensitivity and to overcome this difficulty.

#### 4. Experimental comparison and analysis of the 3D description

In order to evaluate on a realistic case the modelling capability in predicting the ultrasonic propagation disturbances, a specific welded mock-up with calibrated flaws has been manufactured by EDF. Side drilled holes (SDH) and notches were machined in and around the weld (see figure 6). This specific case of SMAW weld has been realized in vertical position. It is important to note that the X-Ray diffraction analysis highlights the disorientation of the fiber axis along the welding direction (about  $18^\circ$ )<sup>(1)</sup>. Due to this disorientation, the (XZ) inspection plane is not a symmetry plane of the orthotropic symmetry. So, modeling this configuration requires using 3D simulation code in order to predict beam deviation out of the incidence plane.

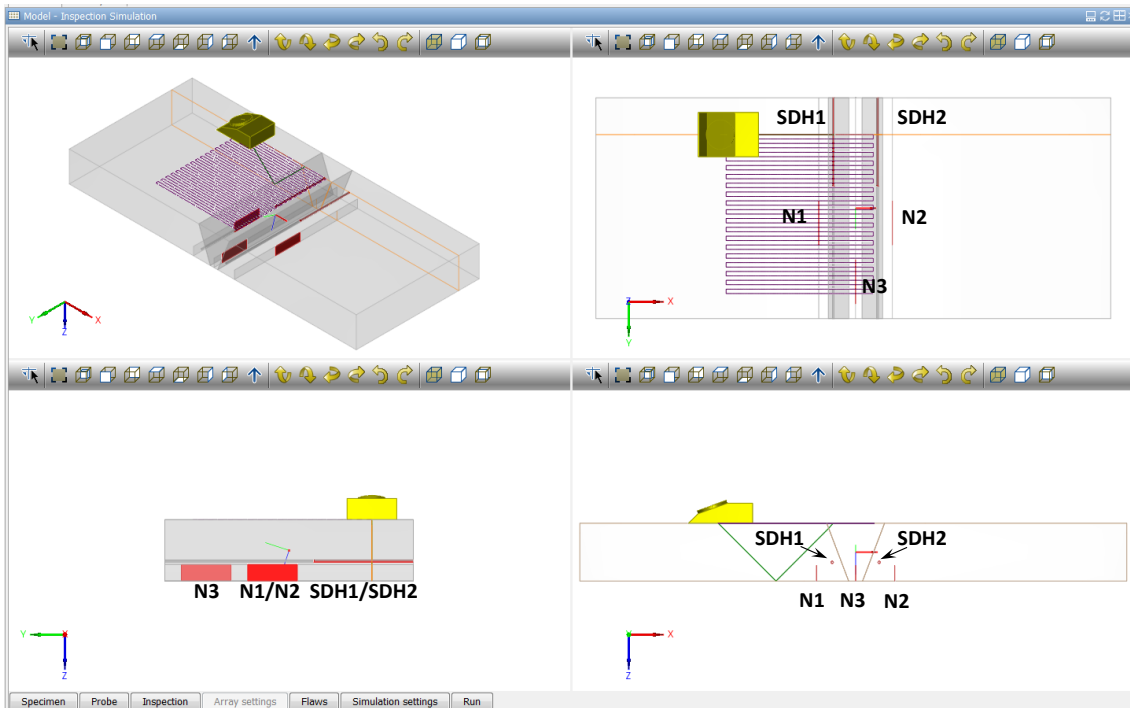


**Figure 6. Representation in CIVA of the inspected mock-up containing SDH and notches in and around a specific case of SMAW weld realized in vertical position with disorientation of the fiber axis in the (YZ) plane about  $18^\circ$ .**

We have chosen to study an experimental inspection on a specific SMAW weld performed by using a 2 MHz piezoelectric transducer mounted on PMMA wedge to generate longitudinal waves at  $45^\circ$ . The sample has been machined to provide a flat surface for inspection and is 37 mm thick. Characteristics of inspected flaws are the following:

- two side-drilled holes (SDH) located at a 25 mm depth in the base metal near the weld, on the left side (SDH1) and right side (SDH2) at 15 mm from the middle of the welding joint. Their length is about 60 mm and their diameter is 1.5 mm.

- three notches of 10 mm height and 30 mm length. Two of them are located in the base metal near the weld, on the left side (N1) and right side (N2) at 25 mm from the middle of the welding joint. The third N3 is located in the middle of the weld.

We present comparison of the DRT simulation for three inspection planes. The first, denoted inspection plane 1 (IP1), contains only SDH1 and SDH2 echoes. The second, denoted IP2, provides the ultrasonic responses of notches N1 and N2. The last, denoted IP3, aims at studying the notch N3 located in the weld. These planes are identified on the CScan image illustrated in figure 7.

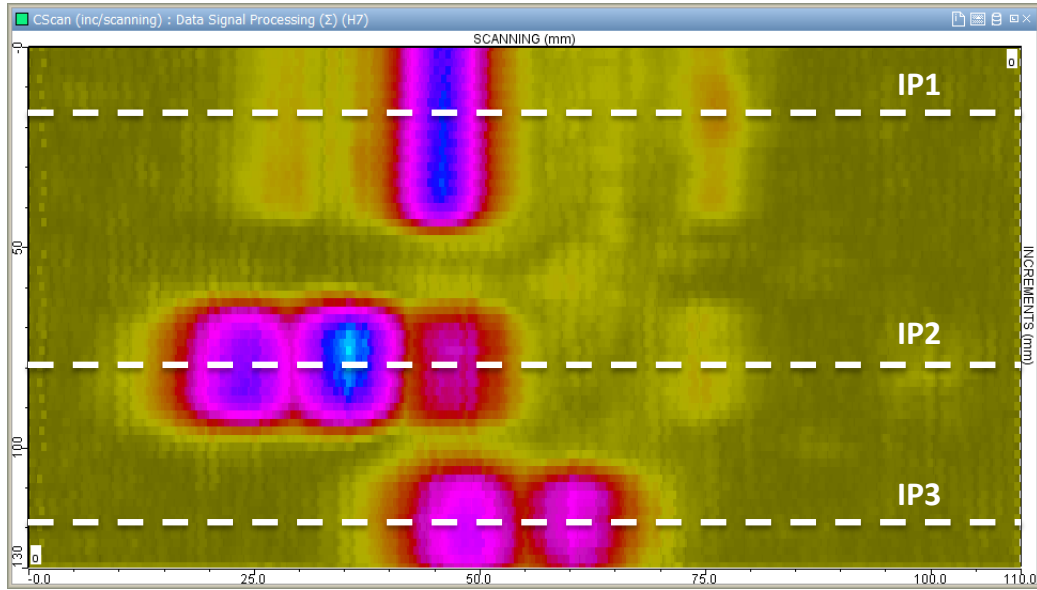


**Figure 7. Experimental CScan and identification of the different planes of inspection studied thereafter.**

From a general point of view, simulation results show that the influence of the disorientation about  $18^\circ$  of the grain orientation out of the plane of inspection is not predominant for L45 wave inspection. Indeed, the variation amplitude of echoes is less than 1 dB in any cases. It was rather the attenuation data of the weld that play a main role in decreasing amplitude echoes about 4 to 5 dB.

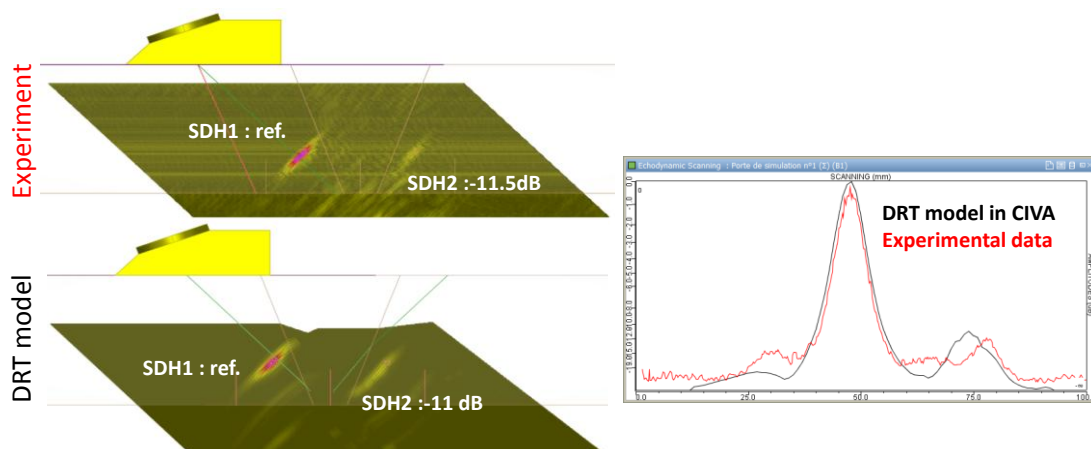


**Figure 8. BScan comparison of experimental and DRT simulated inspections in IP1 plane (SDH1/SDH2 echo analysis).**

In the IP1 plane (see figure 8), the SDH echoes can be analysed. The comparison between the experimental and simulated data provides a very good agreement of direct echoes before and after passing through the welding joint. The experimental decreasing is around 11.5 dB and the simulated one is estimated to 11 dB.

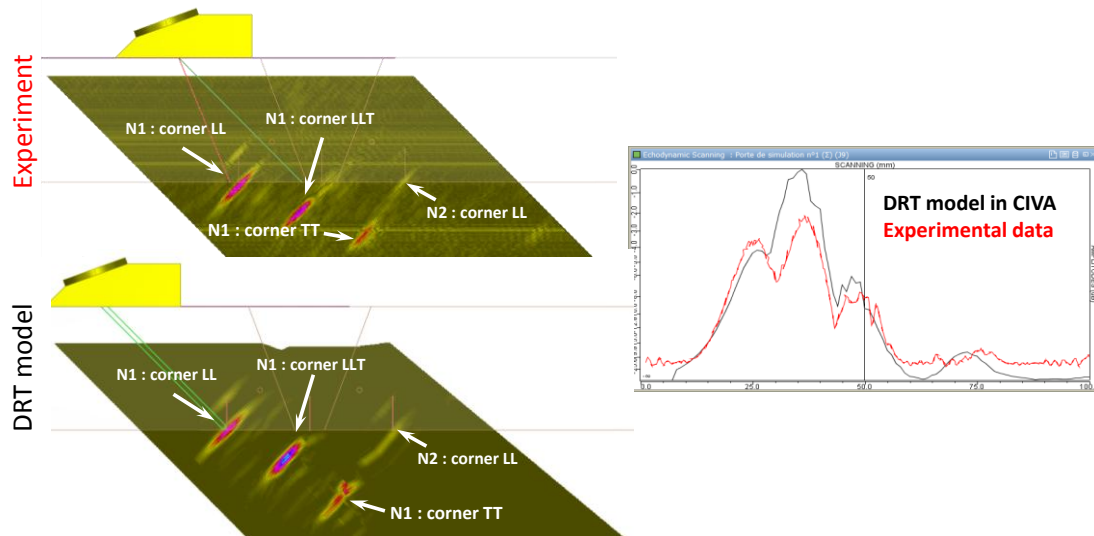


**Figure 9. BScan comparison of experimental and DRT simulated inspections in IP2 plane (N1/N2 echo analysis)**

Concerning the IP2 inspection plane (see figure 9), a particular attention is paid to the corner echoes observed in this case. If the simulated mixed corner echo (LLT) of N1 notch seems to be overestimated with respect to other corner echoes, the comparison between the experimental and simulated signals gives a good agreement especially for the LL corner echo. Note that if the mixed echo is the main one before the weld joint, the signal of the same echo after the welded joint is buried in noise structure. The simulation of the qT mode conversion in the weld is not yet well-performed in smoothly anisotropic structure when degenerate modes can be present. In order to treat the problem, an improvement of the qT mode monitoring must be realized during the calculation process of the ray trajectory.

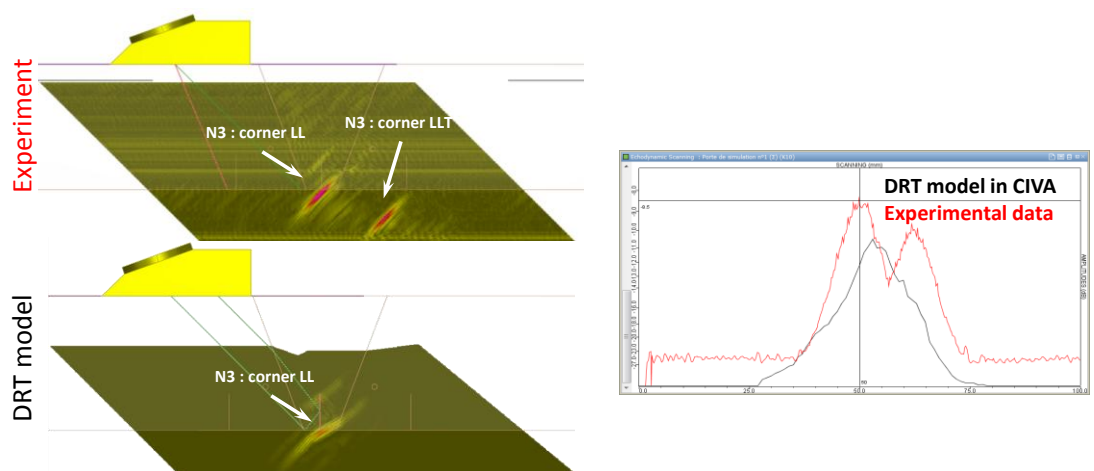


**Figure 10. BScan comparison of experimental and DRT simulated inspections in IP3 plane (N3 echo analysis)**

Finally the worse result concerns the simulation on notch N3 inside the weld in the IP3 inspection plane (see figure 10). A 4 dB discrepancy is observed for the LL corner echo. Different reasons can explain this result. Especially, the description of the weld seam is not enough precise with regards to the inspection of flaws located in this area. A study of the sensitivity of such echoes with respect to variation of material properties near the weld seam has to be done to rule on this point.

## **5. Conclusions**

In this paper, we have presented a part of the MOSAICS project concerning the development of ray-based model dedicated to ultrasonic inspection of welds. In order to treat realistic descriptions of welding joint, the weld can be considered as an unique domain in which the variation of grain orientation is described through a spatial mapping of crystallographic orientations. A new modelling approach using a ray-based approximation on a smoothly inhomogeneous anisotropic medium has been developed. In addition, various GUI tools have been introduced in CIVA to treat such description of welds.

Firstly, this DRT model has been validated for a V-shaped weld described with a closed-form expression. The longitudinal wave field evaluated has been successfully compared with results obtained with the FE code ATHENA. Then, the DRT model has been applied on a V-shaped weld described with a mapping description of the orientations of the grain provided from a macrograph image processing. A good agreement has been observed again. Finally, several comparisons with experimental acquisitions have been done on specific welded mock-up with calibrated flaws. The simulated results, taking account attenuation coefficients in the weld, have shown a very good agreement with experimental data when the flaws are located outside the weld in the base metal. More discrepancies have been observed when the notch is located at the weld seam.

At the current time, a first version of modelling code has been delivered in CIVA to allow simulating complex 3D configurations in terms of probe, defect and material. We are currently working on numerical problems concerning transverse wave propagation in smoothly inhomogeneous anisotropic medium. Concerning the attenuation coefficients, the general anisotropy of the wave attenuation should be handled subsequently before the end of the project. The last improvement focuses on the computation time and the numerical precision by using higher-order numerical methods such as the common fourth-order Runge-Kutta method.

## **Acknowledgements**

This work was realized in the framework of the MOSAICS project (Modelling of an austenitic stainless steel weld inspected by ultrasonic technics) which is supported by the French National Agency of Research.

## **References**

1. B Chassignole et al., '3D modelling of ultrasonic in austenitic welds', in this proceedings.

2. B Chassignole et al., 'Modelling the attenuation in the ATHENA finite element code for the ultrasonic testing of austenitic stainless steel welds', *Ultrasonics*, Vol 49, pp 653-658, 2000.
3. A Apfel et al., 'Coupling an ultrasonic propagation code with a model of the heterogeneity of multipass welds to simulate ultrasonic testing', *Ultrasonics*, Vol 43, pp 447-456, 2005.
4. CIVA software platform for simulating NDT techniques (UT, EC, RT) <http://www-civa.cea.fr>
5. A Lhémercy et al., 'Modeling tools for ultrasonic inspection of welds', *NDT&E Int.*, Vol 37, pp 499-513, 2000.
6. K Jezzine et al., 'Evaluation of ray-based methods for the simulation of UT welds inspection', 39<sup>th</sup> *Review of Progress in QNDE*, Vol 32B, pp 1073-1080, 2013.
7. A Gardahaut et al., 'Modelling tools for ultrasonic inspection of bimetallic welds', *Proceedings of the Acoustics 2012 Nantes Conference*, 2012.
8. V Červený, 'Seismic ray Theory', Cambridge University Press, 2001.
9. A Gardahaut et al., 'Paraxial ray-tracing approach for the simulation of ultrasonic inspection of welds', 40<sup>th</sup> *Review of Progress in QNDE*, to be published.
10. J A Ogilvy, 'Computerized ultrasonic ray tracing in austenitic steel', *NDT International*, Vol 18, pp 67-77, 1985.